JOURNAL OF Applied Polymer SCIENCE

Morphologies of electrospun fibers of lignin in poly(ethylene oxide)/ N,N-dimethylformamide

Samira Aslanzadeh,[1] Behzad Ahvazi,[2] Yaman Boluk,[3,4] Cagri Ayranci[1]
[1]Department of Mechanical Engineering, University of Alberta, Edmonton, Alberta T6G 2G8, Canada
[2]Alberta Innovates–Technology Futures, Edmonton, Alberta T6N 1E4, Canada
[3]Department of Civil and Environmental Engineering, University of Alberta, Edmonton, Alberta T6G 2W2, Canada
[4]National Institute for Nanotechnology, Edmonton, Alberta T6G 2M9, Canada
Correspondence to: C. Ayranci (E-mail: cayranci@ualberta.ca)

ABSTRACT: The effects of polyethylene oxide (PEO) molecular weight (Mv), and volume fraction (ϕ) on the morphology of electrospun sulfur free softwood lignin nanofibers were investigated. Small amounts of PEO were used during preparations of the solutions to aid the electrospinning process. It was found that tripling the PEO volume fraction resulted in a transition from semi-dilute unentangled to semi-dilute entangled solutions. Conversely, the solution remained in the semi-dilute un-entangled regime as the molecular weight was increased by five times. The effects of molecular weight and volume fraction of PEO both on entanglement density and fiber morphology were unified by scaling PEO viscosities as a function of $\left(\phi^{1.3}Mv\right)_{\text{polymer}}$. We investigated and discussed conditions that would produce smooth fibers and conditions that would produce fibers with beads. In the case of beads-on-a-string formation, bead widths remained constant regardless of the molecular weight and concentration of PEO, but the bead length changed. Additionally, we observed a decrease in the diameter of the fibers and the dimension of beads (length and width of beads) with an increase in the electric field used for electrospinning. The aspect ratio of beads increased with increases to both the electric field and the PEO molecular weight or concentration. © 2016 Wiley Periodicals, Inc. J. Appl. Polym. Sci. **2016**, *133*, 44172.

KEYWORDS: biopolymers and renewable polymers; electrospinning; fibers

Received 17 May 2016; accepted 10 July 2016
DOI: 10.1002/app.44172

INTRODUCTION

In an electrospinning process, polymer solutions are subjected to an electric field resulting in an electrically charged jet that travels from a spinneret toward a grounded collector. After the formation of the jet stream in an almost straight line, it bends into a disordered path, called a whipping jet.[1] This whipping jet is stretched and thinned by electrical forces, during which time the solvent evaporates, and micro- and nanofibers are deposited onto the collector. In electrospinning, the Rayleigh capillary and bending instabilities (also called whipping instability by some researchers)[1] are two main factors which determine the quality of the fibers formed (beaded fibers or smooth fibers).[1]

The capillary instability is governed by surface tension. The surface tension tends to minimize the free surface energy and the surface area of the air–liquid boundary. This tendency causes the formation of axially symmetric perturbations which break up the jet into a series of droplets or a beads-on-a-string (BOAS) structure.[1,2] To produce bead-free and uniform fibers, the Rayleigh capillary instability has to be suppressed by viscoelastic forces. For example, increasing the concentration and molecular weight of polyethylene oxide (PEO) in water solution enhances the viscoelastic forces of the solution.[3] The competition between the surface tension and viscoelastic forces results in the different fiber morphologies,[4] such as beads-only, BOAS[5,6] (or beaded fibers), and bead-free fibers (i.e., smooth fibers).

The formation of beads-only (or droplets) is due to the lack of viscoelastic forces, which is called the electrospraying process.[1] A strong elongational flow can completely stretch macromolecular chains leading to a smooth fiber.[1,7] However, the formation of the BOAS morphology is attributed to the coil-stretch transition of the macromolecules.[1] In BOAS morphology, there are tiny strings or threads between the beads. These strings are formed due to the resistance of the liquid jet to any further deformation.[1]

The bead formation on the electrospun fibers is an unfavorable defect or "by-product"[4] in the electrospinning process.

Additional Supporting Information may be found in the online version of this article.

Mechanisms of the bead formation and obtaining bead-free fibers are available in the literature.[3,4,8–10] To investigate the bead morphology, we must investigate the *average length*, *width*, and the corresponding *aspect ratio* (the ratio of bead length to bead width) of the beads. Further, the *average wavelength of the bead-forming instability* needs to be investigated[4,11,12] where *Wavelength of the bead-forming instability* is defined as the distance between the centers of two beads.[9,13]

The bending instability is divided into two: electric field induced axisymmetric and non-axisymmetric whipping (or bending) instabilities.[14–17] The competition between these instabilities also determines the quality of electrospun products (BOAS or bead-free fibers).

Two of these three instabilities are axisymmetric (i.e., electric field induced axisymmetric bending instability and Rayleigh capillary instability), where the jet axis stays constant, but the radius of the jet varies along the jet axis. Conversely, for the electric field induced non-axisymmetric whipping the radius of the jet is stable, but the jet axis fluctuates.[1,13] Beads form in the axisymmetric instabilities mode, while the increased whipping instability helps the reduction of bead formation. For instance, the addition of salt to PEO/water solution causes the net charge density and electrical forces increase.[4,18]

It has been determined by other research groups that high molecular weight PEO facilitates the electrospinning process because of its unique viscoelastic properties.[3,18–20] Several research groups investigated the electrospinning of lignin.[21–28] These studies demonstrated that the addition of PEO to lignin suspension aids the production of good quality fibers during the electrospinning process.[22]

The purpose of this article is to investigate the role of PEO concentration and molecular weight (Mv) in forming bead-free fibers using lignin. Here, we are expanding on our previous study[29] to consider the effect of PEO molecular weight, as well as concentration, on BOAS morphologies. In particular, we investigate the formation of beads during electrospinning and evolution of the shape of the beads until uniform (bead-free) fibers have formed. Production of bead-free fibers is necessary when lignin is used as a precursor for carbon fiber production because beads reduce mechanical properties of the fibers. Only a few groups have previously considered the change of bead morphology with the polymer solution properties and processing variables and these studies were undertaken with different polymers.[4,11,12] To the best our knowledge, the present study is the first to consider and interpret the effects of the concentration and the molecular weight of a macromolecular polymer like PEO on bead morphology.

EXPERIMENTAL

Materials

Sulfur-free softwood lignin (SFSL) was provided by Alberta innovates technology futures (AITF), Edmonton, AB, Canada. SFSL was extracted from pin chips received from a kraft pulp mill by using the supplier's own proprietary lignin extraction and purification processes. PEO with molecular weights, Mv of 1,000, 2,000, and 5,000 kD were purchased from Sigma Aldrich. Molecular Biology Grade, anhydrous N,N-dimethylformamide (DMF), purchased from Sigma Aldrich, was used as the solvent without any further treatment for the preparation of the SFSL/electrospinning solutions.

Preparation of Spinning Solutions and Electrospinning Mats

Electrospinning solutions were prepared as previously described.[29] Three series of SFSL/PEO solutions with total solid volume fractions of 0.32, 0.42, and 0.48 were investigated, while using three different PEO molecular weight samples (1,000, 2,000, and 5,000 kDa) in each series. Electrospinning setup, consisted of a flat-tip 20G needle with a constant working distance (tip-to-collector distance) of 0.2 m. The flow rate was 4.2×10^{-10} m^3/s. The collector was a stationary type collector. The SFSL/PEO solution compositions, applied electric field and fiber morphologies were summarized in Tables (I–III).

Characterization

We examined the electro-spun fibers using the VEGA3 RESCAN Field Emission scanning electron microscope (SEM), with gold-coated samples and accelerating voltage of 20 kV. At least 100 measurements were taken from the samples to determine fiber/string diameters.[29] Using ImageJ analysis software (NIST), wavelength of the bead-forming instability (λ), and length and width of beads were determined from SEM images by 15 measurements made on each sample that had beads. Later, average and 95% confidence limits were calculated using a *t*-test analysis.

Steady state shear measurements (over the frequency range of 1–100 s^{-1}) and linear oscillatory viscoelastic measurements (over the range of 0.628–628 rad/s) of colloidal SFSL and PEO solutions with and without SLSF were carried out on a combined motor and transducer AR-G2 Rheometer (TA Instruments, New Castle, Delaware, USA). The oscillatory strain was 10%. Sixty millimeter diameter aluminum cone and plate (two nominal angle) geometry were used in measurements. By employing Huggins equation, we used steady state zero shear viscosities to calculate intrinsic viscosities of lignin suspension and PEO solutions.[30] Calculated intrinsic viscosities of SFSL and PEO (Mv of 1,000 kD) in DMF were 9.4×10^{-2} dL/g and 6.7 dL/g, respectively, as explained in Ref. 29. Intrinsic viscosities of SFSL and PEO compares well with those reported in the literature review.[31–33]

Overlap concentration (c^*) and entanglement concentration (c_e) are critical concentrations for predicting the degree of entanglement of polymer chains in solutions.[34] In this research, these concentrations are expressed in terms of volume fractions ($\phi^* = c^*/\rho_{PEO}$ and $\phi_e = c_e/\rho_{PEO}$). The supplier reported the density of the lignin as 550 kg/m^3, and this number was considered in all related calculations in this study. The supplier reported the density of PEO as 1,210 kg/m^3.

RESULTS AND DISCUSSION

Effect of Solution Properties on Bead Morphology

The effects of molecular weight (Mv_{PEO}) and volume fraction (ϕ_{PEO}) of PEO on the stability and the morphology of SFSL electro-spun fibers are summarized in Tables (I–III).

Figure 1 shows the SEM pictures of the electrospun materials (BOAS and uniform bead-free fibers) over the specified Mv_{PEO}

Table I. Electrospinning SFSL/PEO Solution Composition and the Resulting Electrospun Products at Total Solid (SFSL/PEO) Volume Fraction of 0.32 (concentration of 22.0 wt %)

PEO Mv	PEO volume fraction	PEO concentration (wt %) in PEO/SFSL/DMF solution	Shear viscosity (Pa s)	PEO/SFSL in dry fiber	Electric field (kV/m)	Morphology	Fiber/string diameter (nm)
1,000 kDa[a]	0.0075	1.1	0.0802	5/95	50	Bead-free Fiber	1093 ± 28
					60	Bead-free Fiber	1028 ± 21
					70	Bead-free Fiber	968 ± 20
	0.0060	0.88	0.0436	4/96	50	Bead-free Fiber	750 ± 20
					60	Bead-free Fiber	727 ± 15
					70	Bead-free Fiber	671 ± 17
	0.0045	0.66	0.0295	3/97	60	Bead-free Fiber	667 ± 12
	0.0037	0.55	0.0259	2.5/97.5	70	BOAS[a]	559 ± 22
	0.0030	0.44	0.0171	2/98	70	BOAS[a]	418 ± 28
	0.0015	0.22	0.0108	1/99	70	BOAS[a]	180 ± 37
2,000 kDa	0.0015	0.22	0.0131	1/99	70	BOAS[a]	644 ± 38
5,000 kDa	0.0015	0.22	0.0159	1/99	50	BOAS[a]	882 ± 40
					60	BOAS[a]	860 ± 39
					70	BOAS[a]	736 ± 17

Data corresponding to 1,000 kDa Mv is adopted from Ref. 29.
[a] BOAS: Beads-On-A-String.

and ϕ_{PEO} range as the total solid volume fraction SFSL/PEO; ϕ_T was kept at 0.32.

The transition from beads, to BOAS, and to bead-free fibers that is observed in Figure 1 is converted to a schematic representation in Figure 2. In these figures, it is initially observed that increasing the Mv_{PEO} or ϕ_{PEO} altered the morphology of beads from spherical forms into spindle-like ones. By further increasing either Mv_{PEO} or ϕ_{PEO}, the bulge of spindle-like beads disappeared and led to uniform fibers. As the shape of beads changed from spheres to spindle-like, the length of beads increased steadily, while the widths stayed almost constant. This behavior was also observed by Fong *et al.* while reporting the bead formation of electrospun PEO from water solutions.[4] In the meantime, the diameter of the string/thread part was also

Table II. Electro-Spinning SFSL/PEO Solution Composition and the Resulting Electro-Spun Products at Total Solid (SFSL/PEO) Volume Fraction of 0.42 (concentration of 30.0 wt %)

PEO Mv	PEO volume fraction	PEO concentration (wt %) in PEO/SFSL/DMF solution	PEO/S FSL in dry fiber	Electric field (V/m)	Morphology	Fiber/string diameter (nm)
1,000 kDa[a]	0.00192	0.3	1/99	70×10^3	Bead-free Fiber	809 ± 26
	0.00096	0.15	0.5/99.5	70×10^3	BOAS[a]	574 ± 37
2,000 kDa	0.00096	0.15	0.5/99.5	70×10^3	BOAS[a]	632 ± 32
	0.00048	0.075	0.25/99.75	60×10^3	BOAS[a]	581 ± 27
	0.00019	0.03	0.1/99.9	85×10^3	Mixture of Beads/BOAS[a]	—
5,000 kDa	0.00096	0.15	0.5/99.5	70×10^3	Bead-free Fiber	756 ± 19
				80×10^3	Bead-free Fiber	765 ± 20
				90×10^3	Bead-free Fiber	655 ± 18
	0.00048	0.075	0.25/99.75	70×10^3	Bead-free Fiber	912 ± 24
				80×10^3	Bead-free Fiber	789 ± 19
				90×10^3	Bead-free Fiber	694 ± 17
	0.00019	0.03	0.1/99.9	60×10^3	Mixture of Beads/BOAS[a]	—

Data corresponding to 1,000 kDa Mv is adopted from Ref. 29.
[a] BOAS: Beads-On-A-String.

Table III. Electro-Spinning SFSL/PEO Solution Composition and the Resulting Electro-Spun Products at Total Solid (SFSL/PEO) Volume Fraction of 0.48 (concentration of 35.0 wt %)

PEO Mv	PEO volume fraction	PEO concentration (wt %) in PEO/ SFSL/DMF solution	PEO/SFSL in dry fiber	Electric field (kV/m)	Morphology	Fiber/string diameter (nm)
1,000 kDa[a]	0.00219	0.35	1	70	Non-uniform fiber	—
	0.00109	0.175	0.5	70	Bead-free fiber	1111 ± 32
	0.00055	0.0875	0.25	70	Bead-free fiber	970 ± 28
	0.00022	0.035	0.1	70	Mixture of beads/BOAS[a]	—
2,000 kDa	0.00055	0.0875	0.25	70	Non-uniform fiber	—
	0.00022	0.035	0.1	70	BOAS[a]	—
5,000 kDa	0.00055	0.0875	0.25	60	Non-uniform fiber	—
	0.00022	0.035	0.1	60	Non-uniform fiber	—
				70	Non-uniform fiber	—
				80	Non-uniform fiber	—

Data corresponding to 1,000 kDa Mv is adopted from Ref. 29.
[a] BOAS: Beads-On-A-String.

increased. The existence of tiny threads between the beads is named "*long-lived*."[8] In a beaded morphology, thin threads are squeezed radially by the capillary pressure.[1] The increase in the string/thread diameter showed the decrease in the capillary pressure in the liquid jet during electrospinning.

Chain entanglement density of polymers in solutions plays an important role on the morphology of electrospun fibers, and this entanglement density can be changed by changing either the molecular weight (Mv_{PEO}) or the volume fraction (ϕ_{PEO}).[19] The chain entanglement of a polymer solution can be related to its Newtonian-plateau viscosity, which can be used as an indication of the fiber morphology and diameter.[35] Therefore, we investigated the effects of molecular weight (Mv_{PEO}) and the volume fraction (ϕ_{PEO}) of PEO on the morphology of electrospun fibers here by means of suspension/solution viscosities. PEO in DMF solutions and SFSL + PEO in DMF suspensions were Newtonian as the shear viscosities are independent of the shear rate[29] (Supporting Information Figure S1).

Intrinsic viscosities of different molecular weight PEO samples used in this study are summarized in Table IV. This table also

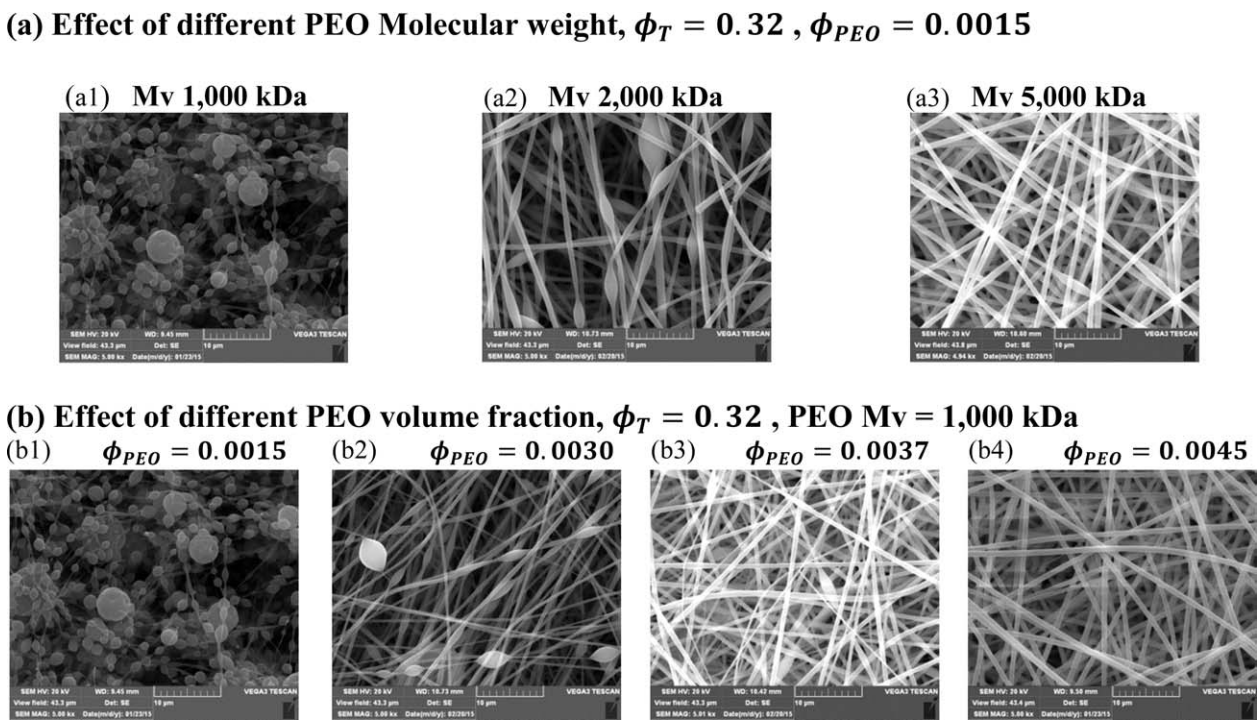

Figure 1. Effect of (a) molecular weight and (b) volume fraction of PEO on bead morphology and related SEM images. The staff guage is 10 μm.

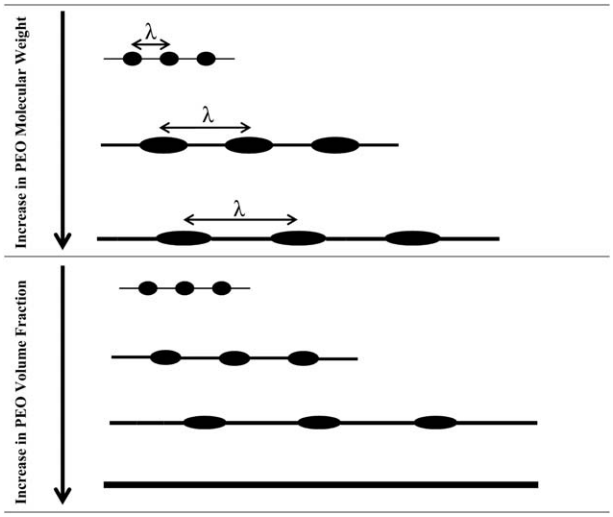

Figure 2. Schematic drawing for the transitions from BOAS to bead-free fibers. λ is the wavelength of the bead-forming instability.

includes overlap volume fraction, ϕ^* and ϕ_{PEO}/ϕ^*at a PEO volume fraction of 0.0015 for different Mv of PEO. The values of ϕ_{PEO}/ϕ^* at volume fraction of 0.0015 for different molecular weights of PEO are less than $\phi_{PEO}/\phi^* \sim 3.6$. The value of 3.6 was the change of viscosity slope while PEO (Mv = 1,000 kDa) volume fraction was increased.[29] As it was reported in our previous publication for the same system, at $\phi_{PEO}/\phi^* = 3.6$ both the viscosity slope change and transition from BOAS to smooth fiber occurred. At ϕ_{PEO}/ϕ^* less than 3.6, the solution was in semi-dilute un-entangled regime.

When we look at the ϕ_{PEO}/ϕ^* values (1.2, 1.3, and 2.4 for the different Mv) in Table IV, they are all lower than the previously determined threshold of $\phi_{PEO}/\phi^* = 3.6$. All of these conditions produced beaded fibers and this is consistent with the expectations. In this regime, PEO chains overlap, but not enough to cause a significant entanglement density. Therefore, one can conclude that the lack of chain entanglements causes beads to form. Our results compared well with the PMMA/DMF electrospun products, where Gupta *et al.* investigated the effect of poly methyl methacrylate concentration and molecular weight on fiber formation during the electrospinning.[36]

As proposed by Grassley, the effects of the PEO molecular weight and concentration on the chain entanglement were unified by scaling PEO viscosities as a function of $\left(\phi^{1.3}\mathrm{Mv}\right)_{polymer}$.[34] We scaled the Newtonian viscosity of PEO in DMF solution by subtracting it from the viscosity of solvent DMF. As a result, we considered only the PEO contribution in the PEO/DMF solution. Figure 3(a) shows the plot of scaled PEO viscosity in DMF $(\eta_{PEO\ in\ DMF} - \eta_{DMF})$ versus $\left(\phi^{1.3}\mathrm{Mv}\right)_{PEO}$. The same approach was also used in the case of PEO solutions in SFSL/DMF suspensions by plotting $(\eta_{(SFSL+PEO)in\ DMF} - \eta_{SFSL\ in\ DMF})$ as a function of $\left(\phi^{1.3}\ \mathrm{Mv}\right)_{PEO}$ in Figure 3(b). Using the unfilled and filled legends, respectively, for each data point on the plot, BOAS and beads-free fibers were marked. In addition, fiber diameter values were also listed next to each data point.

In the case of PEO/DMF solutions, the onset of the entanglement effects on the scaled PEO viscosity appeared at $\left(\phi^{1.3}\mathrm{Mv}\right)_{PEO} \sim 1.45$. On the other side, PEO solutions in SFSL/DMF suspensions showed the slope change at $\left(\phi^{1.3}\mathrm{Mv}\right)_{PEO} \sim 0.9$. Nevertheless, if one excludes the volume of SFSL dispersion in DMF, the apparent $\left[\left(\phi^{1.3}\mathrm{Mv}\right)_{PEO}\right]_{app}$ will be 1.32 by using a simple correction: $(0.9/[1.0 - \phi_{SFSL}])$. Comparison of $\left(\phi^{1.3}\mathrm{Mv}\right)$ of PEO in DMF solution and $\left(\phi^{1.3}\mathrm{Mv}\right)_{app}$of PEO in SFSL/DMF suspension (1.45 vs 1.32) showed that the presence of SFSL did not perturb the entanglement of PEO in DMF. This was due to the absence of any interaction between SFSL dispersion and PEO macromolecules.

Figure 4 shows the data points on the total (SFSL/PEO) volume fractions (ϕ_T) versus $\left(\phi^{1.3}\mathrm{Mv}\right)_{PEO}$ of PEO plot. The unfilled and filled legends represent BOAS and beads-free fibers, respectively. This plot can be divided into two regions: BOAS and beads-free fiber morphologies. This mapping plot demonstrates the minimum value of $\left(\phi^{1.3}\mathrm{Mv}\right)_{PEO}$ to attain bead-free fiber morphology. As shown in Figure 4, by increasing the total (SFSL/PEO) volume fraction, the value of $\left(\phi^{1.3}\mathrm{Mv}\right)_{PEO}$ needed to obtain the beads-free-fiber decreases. The minimum value of $\left(\phi^{1.3}\mathrm{Mv}\right)_{PEO}$ without SFSL particles is around 10.[4] By increasing the total solid volume fraction to 0.48, the value of $\left(\phi^{1.3}\mathrm{Mv}\right)_{PEO}$ decreased down to 0.1. This is most likely due to the decrease in available free volume for PEO chains by increasing the total (SFSL/PEO) volume fractions. Conversely, as the total solid volume fraction was increased from 0.42 to 0.48, the nonuniform fibers were formed (Supporting Information Figure S2). This is what should be expected, due to the increase of shear viscosity of the solution and lack of free volume for PEO chains in DMF. The detailed information for volume fraction of 0.48 is documented in Table III. The nonuniform fibers were also presented by Dallmeyer, where the total solid concentration was 40 wt % and PEO concentration was 0.1 wt %.[23] When $(\mathrm{Mv})_{PEO}$ of 5,000 kDa was used, according to its $\left(\phi^{1.3}\mathrm{Mv}\right)_{PEO}$ value, beads-free fiber was expected. However, that sample produced the BOAS morphology. It was most likely due to the

Table IV. Intrinsic Viscosity ([η]), Overlap concentration (c^*), Overlap volume fraction (ϕ^*), and ϕ_{PEO}/ϕ^*at ϕ_{PEO}=0.0015

PEO Mv (kDa)	Intrinsic viscosity (dL/g)	Overlap concentration (kg/m^3)	Overlap volume fraction	ϕ_{PEO}/ϕ^*
1,000	6.7[a]	1.5	0.00123	1.2
2,000	7.2[b]	1.1	0.00115	1.3
5,000	13.2[b]	0.6	0.00062	2.4

[a] Experimental result Ref. 29.
[b] Calculated based on a simple scale law law, $\eta = 0.00043\ M_v^{0.67}$ (Polymer Handbook, 4th ed., 1999).

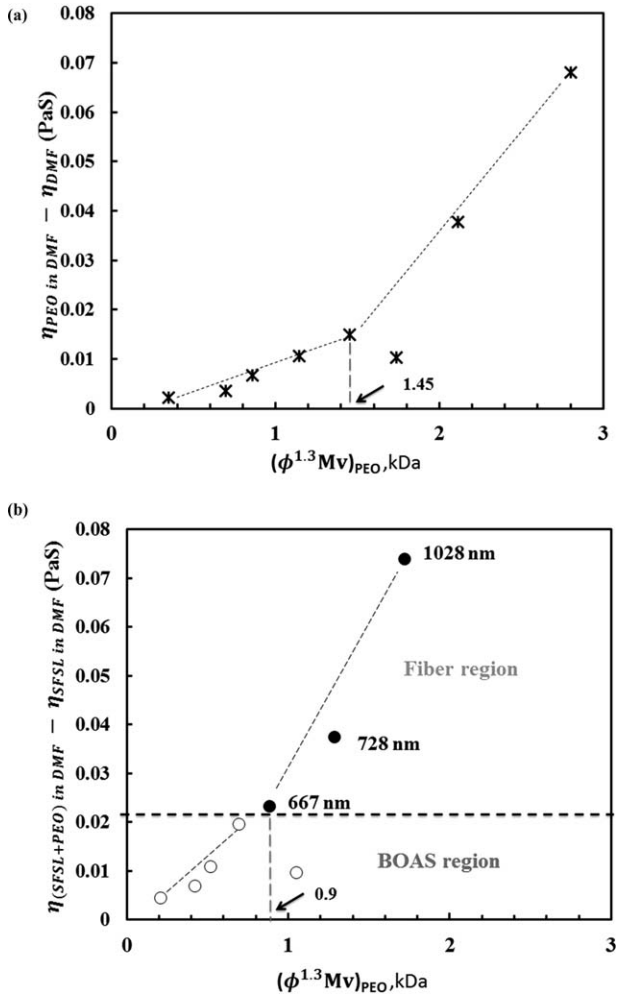

Figure 3. (a) Plot of shear viscosity of $(\eta_{PEO\ in\ DMF} - \eta_{DMF})$ solutions as a function of $(\phi^{1.3}Mv)_{PEO}$ (**b**) Plot of shear viscosity of $(\eta_{SFSL+PEO\ in\ DMF} - \eta_{SFSL\ in\ DMF})$ suspensions and related fiber diameter as a function of $(\phi^{1.3}Mv)_{PEO}$. Filled (•) and unfilled (○) circles mean bead-free fiber and BOAS morphologies, respectively. $\phi_T = 0.32$.

chain scission of 5,000 kDa PEO molecules and generation of lower molecular weight polymer under extensional flow during electrospinning.

The effect of both polymer molecular weight and polymer concentration on morphology of electrospun products was investigated in the literature.[37–39] Based on the results, it can be concluded that the required concentration of the electrospinning solution decreases with the increase in the polymer molecular weight. In SFSL/PEO/DMF suspensions, the higher the SFSL, the less PEO is needed to obtain the bead-free fibers.[29] Palangetic *et al.* proposed the scaling law relating the minimum required concentration of an electrospinning solution to its molecular weight in order to obtain the bead-free fibers.[39] According to the simple scaling law, $\min_{PEO} \sim (M_v)^{-1.16}$ was calculated for SFSL/PEO/DMF suspensions at $\phi_T = 0.42$ and also $\min_{PEO} \sim (M_v)^{-1.75}$ was obtained for SFSL/PEO/DMF suspensions at $\phi_T = 0.48$. A minimum PEO, $\min_{PEO}$, is defined as the minimum PEO volume fraction needed to obtain the bead-free fibers. The detailed information is summarized in Tables II and III. Again, one can conclude that the higher molecular weight of PEO and the higher total solid volume fraction, the less PEO is required.

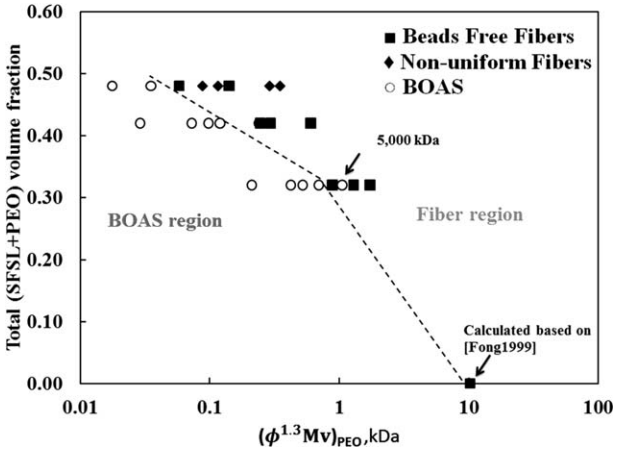

Figure 4. Mapping plot of Total solid volume fraction as a function of $(\phi^{1.3}Mv)_{PEO}$.

The changes of average bead length and bead width versus $(\phi^{1.3}Mv)_{PEO}$ are shown in Figure 5(a). The average bead width remains constant regardless of the PEO molecular weight

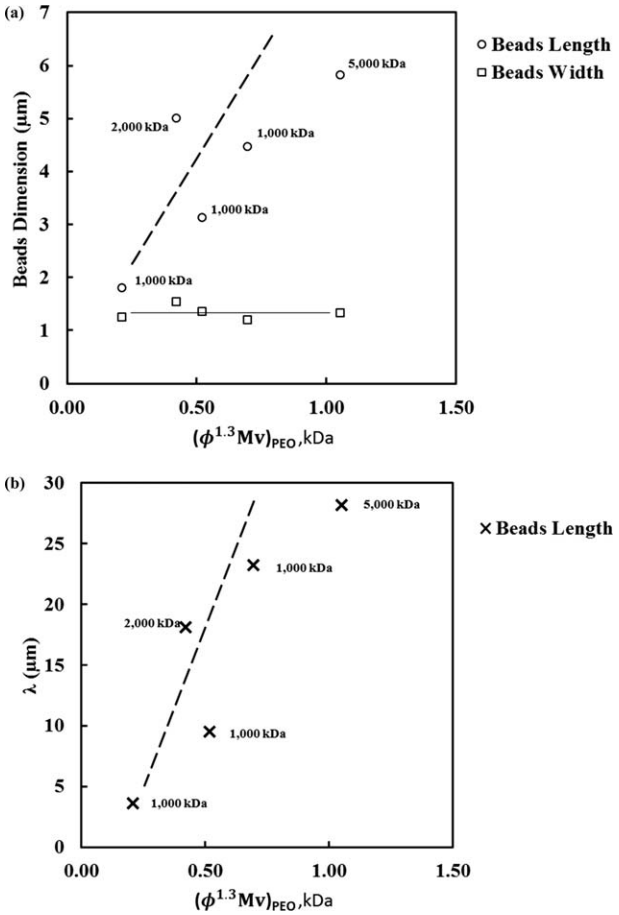

Figure 5. (a) Beads dimension and (**b**) wavelength of the bead-forming instability (λ) as a function of $(\phi^{1.3}Mv)_{PEO}$.

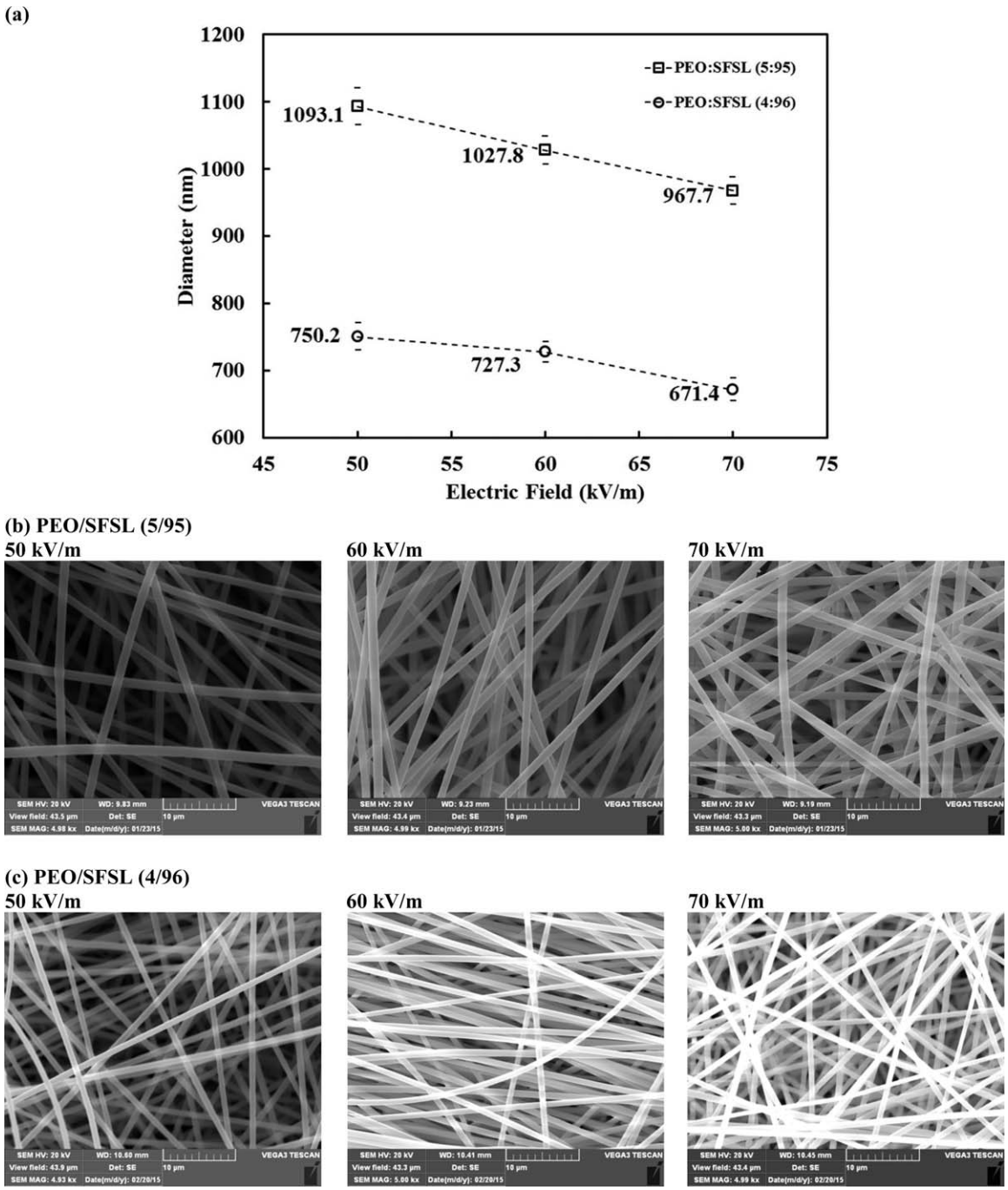

Figure 6. (a) Plot of fiber diameter versus electric field (kV/m); and related SEM images: (b) PEO concentration of 4 wt %; and (**c**) PEO concentration of 5 wt % in mixture of SFSL/PEO. PEO Mv is 1,000 kDa. (−) shows 95% confidence limits. The staff guage is 10 μm.

(Mv_{PEO}) or the PEO volume fraction (ϕ_{PEO}). However, the average bead length increases with the increase in the Mv_{PEO} or ϕ_{PEO}. Thus, by adding higher PEO molecular weight or concentration in the SFSL/DMF suspensions, the extensional viscosities of the solutions increase, causing the beads to be stretched. The jet stream can be subjected to Rayleigh capillary instability, governed by surface tension. The surface tension tends to decrease the surface energy and the surface area of the jet stream. This tendency causes the formation of axially symmetric perturbations. The axisymmetric instability breaks the jet stream into little droplets. In the electrospun fiber formation, the Rayleigh capillary instability has to be suppressed by viscoelastic stresses. As shown in Figure 5(a), increasing viscoelastic stresses are able to overwhelm the bead formation.

The changes of the wavelength of the bead-forming instability (λ) versus $\left(\phi^{1.3}Mv\right)_{PEO}$ are presented in Figure 5(b). The wavelength of the bead-forming instability (λ) increased with the molecular weight or the volume fraction of PEO. The increase in λ demonstrates that Rayleigh instability is suppressed during

Table V. Exponent Dependency between Fiber Diameter (nm) and Electric Field (kV/m)

Polymer System	Reference	Exponent
PEO/SFSL (5/95)		−0.36
PEO/SFSL (4/96)		−0.32
PS/DMF/TEBAC	37	−0.46
PS/DMF/$LiClO_4$	37	−0.61
PAN/carbon nanotube/TiO_2	40	−0.32

transition from BOAS to beads-free fiber. An increase in PEO volume fraction or molecular weight results in suppression of the perturbation growth. As shown in Figure 5(b), increasing viscoelastic stresses are able to increase the wavelength of the bead-forming instability.

Beads-on-fibers were formed during electrospinning of lignin (SFSL) dispersed in PEO/DMF solutions due to the Rayleigh capillary instability. Rayleigh theory indicates that the liquid jets break up into droplets due to the instability of an infinite liquid thread of circular cross section. Conversely, beads disappear if the Rayleigh instability, due to surface tension in the solution, is suppressed completely by viscoelastic forces. Thus, by increasing the molecular weight and volume fraction of PEO, the length and the wavelength of the beads increased, but the width stayed constant while transitioning from beads to uniform fibers. The viscoelastic forces were achieved in the SFSL/DMF suspensions by adding PEO.

At the end of this discussion and as a summary of the Tables (I–III), it can be stated that the morphology of electrospun fibers changed from BOAS to bead-free fibers by tripling the PEO concentration. Conversely, no similar change took place after increasing PEO molecular weight by five times because of lack of chain entanglement density. The bead length increased with increasing PEO molecular weight and concentration, but the increase in PEO molecular weight and concentration had no effect on the bead width.

Effect of Processing Parameters on Bead Morphology

One of the most important processing parameters of electrospinning is the applied voltage and the resulting electric field. In this study, three different voltages were applied with a constant working distance. As expected, in the case of uniform fiber formation, the fiber diameter decreased with the electric field for the samples of PEO/SFSL with 5/95 and 4/96 ratios, as listed in Table I and shown in Figure 6(a). The related SEM images of electrospun fibers can be seen in Figures 6(b) and 6(c).

The dependence of bead-free fiber diameter (D) on electric field for SFSL/PEO along with different polymer systems which were reported in the literature[37,40] is listed in Table V. Values appear in Table V that were calculated using the figures or data provided in the original references. The table shows that diameter (D) versus electric field are scaled with a negative sign of exponents that are similar to the previous findings in the literature. Here, using a simple scaling law, for SFSL/PEO/DMF suspensions it was found that $D \sim (\text{electric field})^{-0.32}$ and $D \sim (\text{electric field})^{-0.36}$ as opposed to $D \sim (\text{electric field})^{-0.46}$ for PS/DMF/TEBAC solution and $D \sim (\text{electric field})^{-0.61}$ for PS/THF/$LiClO_4$ solutions reported in Refs. 37 and 40. However, the effect of the electric field on the fiber diameter is contested in the literature,[2] as there are several studies which reported no noteworthy effect of the electric field on fiber diameter. Further, in some studies, the diameter of the fibers is directly related to the electric field.[2]

Conversely, it was observed that the applied electric field affected the bead morphology of beaded fibers. Figure 7 demonstrates the change of bead morphology with electric field. By rising electric field, the beads convert to smaller and more spindle like shapes.

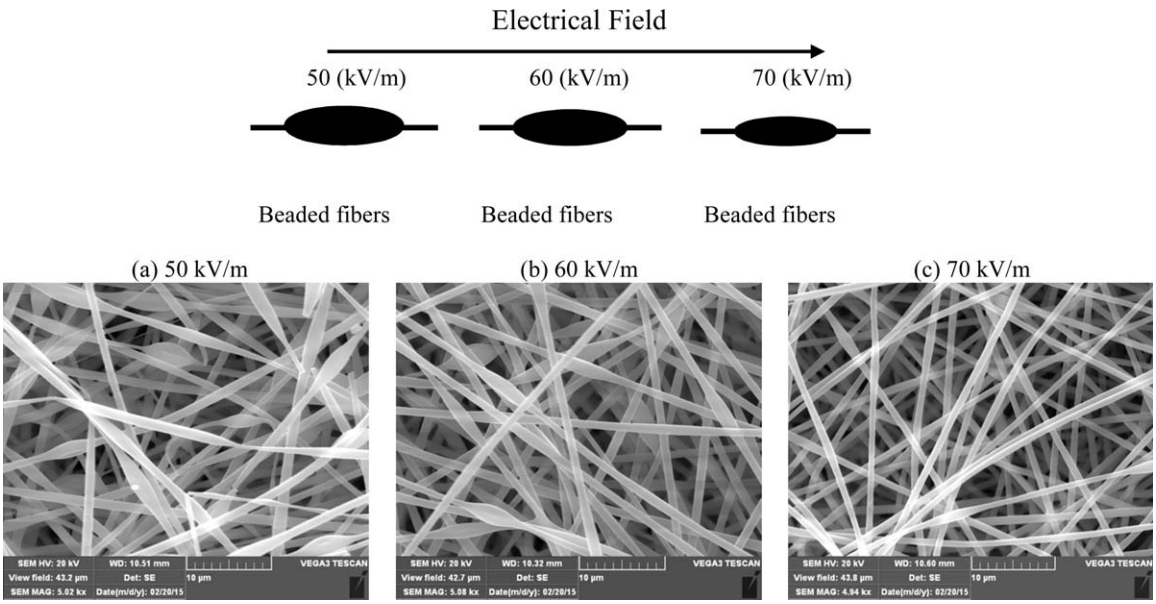

Figure 7. Effect of electric field on bead schematic morphology and related SEM images. ϕ_T=0.32, ϕ_{PEO}=0.0015. PEO Mv is 5,000 kDa (PEO/SFSL concentration of 1/99). The staff guage is 10 μm.

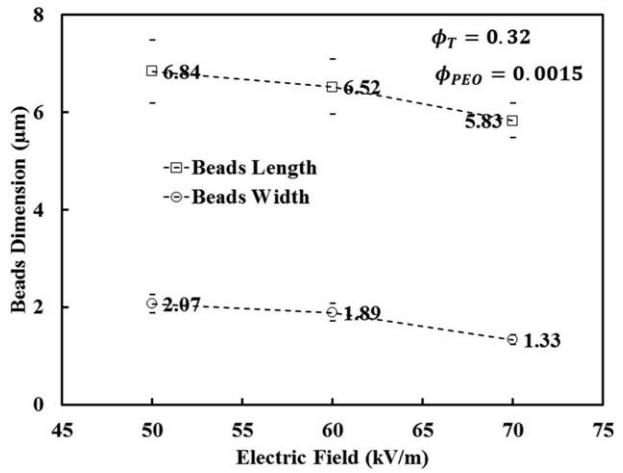

Figure 8. Beads dimension versus electric field (kV/m). ϕ_T=0.32, ϕ_{PEO}=0.0015. PEO Mv is 5,000 kDa (PEO/SFSL concentration of 1/99). (−) shows 95% confidence limits.

The bead dimensions, both bead length and bead width, decreased by increasing the applied electric field (Figure 8). Hence, the bead aspect ratio increased with the electric field from 3.4 to 4.4. Consequently, higher electric field helps to stretch the beads to be stretched. In other words, increasing the aspect ratio indicates the stretching of the beads. Nevertheless, at PEO/SFSL concentration of 1/99, increasing the electric field did not eliminate beads.

CONCLUSIONS

PEO was successfully used as an electrospinning process aid at minimum quantities for the uniform bead-free fiber production from SFSL/DMF suspensions. The effects of PEO molecular weight (Mv) and volume fraction (ϕ) on the morphology of electrospun SFSL nanofibers were investigated. It was found that increasing the PEO molecular weight and PEO volume fractions have similar effects on the morphology of the beaded fibers. By tripling the PEO volume fraction, the BOAS transitioned to bead-free fibers. This transition did not happen after increasing PEO molecular weight by five times due to lack of chain entanglements density. Hence, the effects of molecular weight and concentration of PEO on fiber morphology were unified by scaling PEO viscosities as a function of $(\phi^{1.3}\mathrm{Mv})_{\mathrm{polymer}}$. SFSL in DMF suspensions were found to have no interaction with PEO macromolecules, and the fiber morphology was controlled totally by PEO macromolecules.

It was determined that the bead width was not affected from the changes in PEO molecular weight and concentration. Conversely, the bead length increased with increasing PEO molecular weight and PEO concentration. Finally, when the electric field was increased, a decrease in the diameter of the fibers was also observed, and the bead width and the bead length decreased. The aspect ratio of beads increased with the increasing electric field. This suggested that a higher electric field helps the beads to elongate.

ACKNOWLEDGMENTS

The authors would like to acknowledge funding provided by Alberta Innovates Bio-Solutions (Funding Number: ABI-14-001/RES0022603) for the completion of this research project. Additionally, the authors would like to also acknowledge the in-kind support provided during this project by AITF and National Institute for Nanotechnology (NINT) in Edmonton, AB, Canada. Authors would like to thank Hale Oguzlu for helping in rheology measurements.

REFERENCES

1. Yarin, A. L.; Pourdeyhimi, B.; Ramakrishna, S. Fundamentals and Applications of Micro and Nanofibers; Cambridge University Press: Cambridge, UK, **2014**.
2. Andrady, A. L. Science and Technology of Polymer Nanofibers; Wiley: Hoboken, New Jersey, USA, **2008**.
3. Yu, J. H.; Fridrikh, S. V.; Rutledge, G. C. *Polymer* **2006**, *47*, 4789.
4. Fong, H.; Chun, I.; Reneker, D. H. *Polymer* **1999**, *40*, 4585.
5. Tomczak, N.; van Hulst, N. F.; Vancso, G. J. *Macromolecules* **2005**, *38*, 7863.
6. Oliveira, M. S. N.; Yeh, R.; McKinley, G. H. *J. Non-Newtonian Fluid Mech.* **2006**, *137*, 137.
7. De Gennes, P. *J. Chem. Phys.* **1974**, *60*, 5030.
8. Bhat, P. P.; Appathurai, S.; Harris, M. T.; Pasquali, M.; McKinley, G. H.; Basaran, O. A. *Nat. Phys.* **2010**, *6*, 625.
9. Reneker, D. H.; Yarin, A. L. *Polymer* **2008**, *49*, 2387.
10. Zuo, W.; Zhu, M.; Yang, W.; Yu, H.; Chen, Y.; Zhang, Y. *Polym. Eng. Sci.* **2005**, *45*, 704.
11. Zheng, J.; He, A.; Li, J.; Xu, J.; Han, C. C. *Polymer* **2006**, *47*, 7095.
12. Lee, K. H.; Kim, H. Y.; Bang, H. J.; Jung, Y. H.; Lee, S. G. *Polymer* **2003**, *44*, 4029.
13. Huebner, A.; Chu, H. *J. Fluid Mech.* **1971**, *49*, 361.
14. Hohman, M. M.; Shin, M.; Rutledge, G.; Brenner, M. P. *Phys. Fluids* **2001**, *13*, 2201.
15. Hohman, M. M.; Shin, M.; Rutledge, G.; Brenner, M. P. *Phys. Fluids* **2001**, *13*, 2221.
16. Shin, Y. M.; Hohman, M. M.; Brenner, M. P.; Rutledge, G. C. *Polymer* **2001**, *42*, 09955.
17. Shin, Y. M.; Hohman, M. M.; Brenner, M. P.; Rutledge, G. C. *Appl. Phys. Lett.* **2001**, *78*, 1149.
18. Helgeson, M. E.; Grammatikos, K. N.; Deitzel, J. M.; Wagner, N. J. *Polymer* **2008**, *49*, 2924.
19. Shenoy, S. L.; Bates, W. D.; Frisch, H. L.; Wnek, G. E. *Polymer* **2005**, *46*, 3372.
20. Jin, H. J.; Fridrikh, S. V.; Rutledge, G. C.; Kaplan, D. L. *Biomacromolecules* **2002**, *3*, 1233.
21. Dallmeyer, I.; Chowdhury, S.; Kadla, J. F. *Biomacromolecules* **2013**, *14*, 2354.
22. Dallmeyer, I.; Ko, F.; Kadla, J. F. *J. Wood Chem. Technol.* **2010**, *30*, 315.

23. Dallmeyer, I.; Ko, F.; Kadla, J. F. *Ind. Eng. Chem. Res.* **2014**, *53*, 2697.
24. Dallmeyer, I.; Lin, L. T.; Li, Y.; Ko, F.; Kadla, J. F. *Macromol. Mater. Eng.* **2014**, *299*, 540.
25. Goudarzi, A.; Lin, L. T.; Ko, F. K. *J. Nanotechnol. Eng. Med.* **2014**, *5*, 021006.
26. Lallave, M.; Bedia, J.; Ruiz-Rosas, R.; Rodríguez-Mirasol, J.; Cordero, T.; Otero, J. C.; Marquez, M.; Barrero, A.; Loscertales, I. G. *Adv. Mater.-Deerfield Beach Then Weinheim* **2007**, *19*, 4292.
27. Ruiz-Rosas, R.; Bedia, J.; Lallave, M.; Loscertales, I. G.; Barrero, A.; Rodríguez-Mirasol, J.; Cordero, T. *Carbon* **2010**, *48*, 696.
28. Poursorkhabi, V.; Mohanty, A. K.; Misra, M. *J. Appl. Polym. Sci.* **2015**, *132*, DOI: 10.1002/app.41260.
29. Aslanzadeh, S.; Zhu, Z.; Luo, Q.; Ahvazi, B.; Boluk, Y.; Ayranci, C. *Macromol. Mater. Eng.* **2016**, *301*, 401.
30. Pamies, R.; Hernández Cifre, J.; del Carmen López Martínez, M.; García de la Torre, J. *Coll. Polym. Sci.* **2008**, *286*, 1223.
31. Dong, D.; Fricke, A. L. *Polymer* **1995**, *36*, 2075.
32. Glasser, W. G.; Davé, V.; Frazier, C. E. *J. Wood Chem. Technol.* **1993**, *13*, 545.
33. Kawaguchi, S.; Imai, G.; Suzuki, J.; Miyahara, A.; Kitano, T.; Ito, K. *Polymer* **1997**, *38*, 2885.
34. Graessley, W. W. Polymeric Liquids and Networks: Dynamics and Rheology; Garland Science, New York, USA, **2008**.
35. Zander, N. E. *Polymers* **2013**, *5*, 19.
36. Gupta, P.; Elkins, C.; Long, T. E.; Wilkes, G. L. *Polymer* **2005**, *46*, 4799.
37. Wang, C.; Hsu, C. H.; Lin, J. H. *Macromolecules* **2006**, *39*, 7662.
38. Srinivasan, S.; Chhatre, S. S.; Mabry, J. M.; Cohen, R. E.; McKinley, G. H. *Polymer* **2011**, *52*, 3209.
39. Palangetic, L.; Reddy, N. K.; Srinivasan, S.; Cohen, R. E.; McKinley, G. H.; Clasen, C. *Polymer* **2014**, *55*, 4920.
40. Kedem, S.; Schmidt, J.; Paz, Y.; Cohen, Y. *Langmuir* **2005**, *21*, 5600.